07;08

Size quantization and charge instability in colloidal quantum dots of narrow-gap semiconductors

© S.A. Sergeev, M.V. Gavrikov, N.D. Zhukov

Saratov National Research State University, Saratov, Russia
E-mail: ndzhukov@rambler.ru

Received December 23, 2021
Revised March 1,2022
Accepted March 16,2022

According to the current-voltage characteristics (CVC) and absorption spectra of colloidal quantum dots QD-InSb, -PbS, -HgSe on random samples, the manifestations of charge instability appear in the form of single current peaks and quasi-periodic deviations from the monotonic dependence of the CVC, are determined and studied. The results are explained by dimensional electron quantization in the model of a deep extended potential well and depending on the ratios of the quantization size and the de Broglie wavelength for an electron. It is assumed that the manifestation of Bloch oscillations has been experimentally confirmed. The data on the studied processes are determined and summarized in a table.

Keywords: Quantum dot, nanocrystal, size quantization, quantum selection, Coulomb constraint, Bloch oscillations.

DOI: 10.21883/TPL.2022.05.53472.19115

Most of the scientific publications on the synthesis and properties of colloidal quantum dots (QD) are devoted to variants based on relatively broadband semiconductors, primarily cadmium chalcogenides, which is due, in particular, to their use as photoluminophores [1–3]. In recent years, however, interest in QD based on narrow-zone and gapless semiconductors has increased, which could significantly expand their applications. The positive feature of these QD variants is their high dimensional quantization parameters due to the extremely small values of the effective mass of charge carriers. For full physical manifestation and practical use of size quantization, quantum dots should have an extremely low size dispersion in a wide range of their values, a perfect crystal structure, a properties-controlled surface (such QDs are called nanocrystals) [4]. Production of nanocrystals, however, is complicated by a number of problems. Particularly, in process of growth at synthesis, the size of a perfect nanocrystal is limited by the change in its surface energy decreasing to the van der Waals energy value, when uncontrolled attachment of „foreign" atoms and molecules to the nanocrystal begins [5]. Besides, the narrower the width of the bandgap, i.e. the greater the lattice constant and the lower the binding energy of the atoms therein, the smaller the limiting dimensions of $a_{\max}$ nanocrystal. According to the estimate similar to that in [5], for QD-PbS $a_{\max} \sim 6$ nm, for QD-InSb $a_{\max} \sim 5$ nm, for QD-HgSe $a_{\max} \sim 4$ nm.

Size quantization in QD is a fundamental phenomenon that determines their properties and specifies their features. One of such features is an oscillating nature of photoluminescence level, which is considered in detail in the literature review made in [6]. Electron passage through a quantum dot results in current oscillation caused by charge instability, which is confirmed by theory [7–9] and experiments [10,11]. However, while the features of photoluminescence properties of practical importance for applications in luminophores have been studied in a large number of papers, the publications on current oscillations and charge instability are few, although they are important for science and applications in nanoelectronics.

In connection with the above, this paper studied the influence of size quantization on the electron transport properties, and to confirm its quantum nature, absorption spectra of IR radiation were compared in QD of narrow-gap semiconductors: lead sulfide, indium antimonide and mercury selenide.

The semiconductor parameters used in this paper are: bandgap width E_g, ratio of effective electron mass m to free electron mass m_0, lattice constant a_0. For PbS $E_g \sim 0.41$ eV, $m/m_0 \sim 0.08$, $a_0 \sim 0.593$ nm; for InSb — $E_g \sim 0.17$ eV, $m/m_0 \sim 0.013$, $a_0 \sim 0.649$ nm; for HgSe — $E_g \sim 0.07$ eV, $m/m_0 \sim 0.045$, $a_0 \sim 0.585$ nm [12]. Correct application of bulk semiconductor parameters to nanoparticles is proved, as usual, by correspondence of the relationships of the obtained results, in particular the energy and effective mass of the electron [7,11,13,14].

The samples were made according to the technology described in our papers [5,13], with the selection of the necessary conditions for different variants of the compositions. Each batch of samples was controlled on a random QD sample by scanning electron microscopy (for stoichiometric composition) and transmission electron microscopy (TEM) (for shape and size). Nanocrystal samples of polygonal faceted shape with minimal median dispersion ($\pm 5\%$ max.) were selected for measurements (Fig. 1, *a*).

The study was carried out on the basis of current-voltage curves (CVC) measured by the method of scanning probe microscopy described and developed in our papers [11,14].

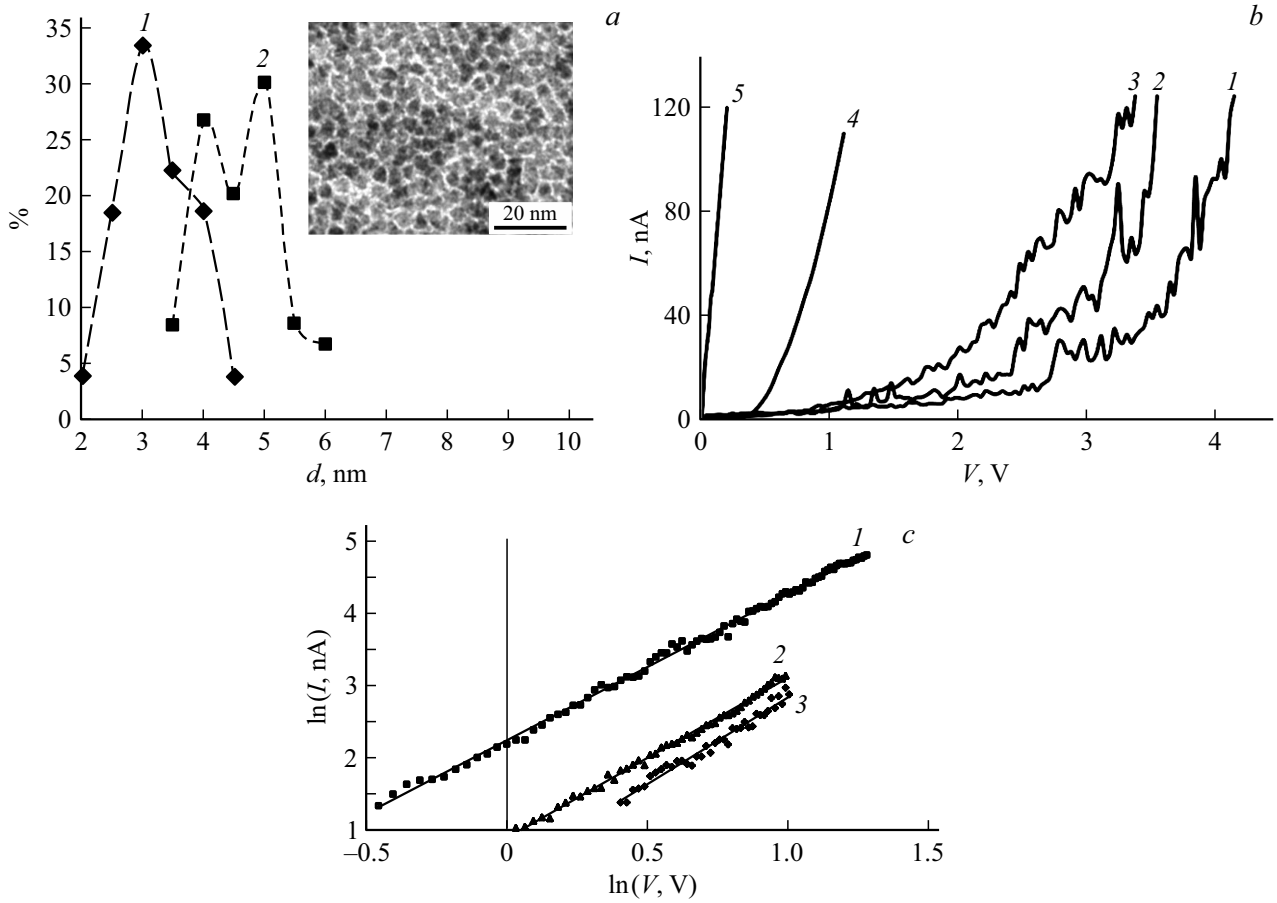

Figure 1. *a* — typical distribution by size and fragmentary TEM-shot (inset). *b* — typical CVC: *1* — InSb, *2* — HgSe, *3* — PbS, *4* — test sample of micro-InSb, *5* — test-sample of ITO; *c* — compliance of dependence $I \sim V^{\beta}$: *1* — PbS, $\beta \sim 2.04$; *2* — HgSe, $\beta \sim 2.25$; *3* — InSb, $\beta \sim 2.41$.

Immediately before the measurements the QDs were made free from ligands by sediment detachment through centrifugation and redispersion in chloroform or ethanol and set out as an island monolayer on a glass substrate with a conducting layer of indium-tin oxide (ITO) using the technology of the Langmuir–Blodgett films [15]. In each sample at least 20 points-particles of random samples were measured. For each of three types of samples a total of at least 150 points-particles were measured. Absorption spectra were measured on FTIR spectrometer IRAffinity-1 (Shimadzu Corp., Japan). Samples for measurements were prepared by deposition on a silicon substrate by a drop method with a prolonged drying with heating.

The size quantization properties in QD are defined by the nature of electron motion therein described by the Schrodinger's equation. The literature has accumulated large theoretical material for various options of quantum-size structures (see, for instance, papers [7,8,16,17]). Use of simplifying models finds solutions in the form of a wave function Ψ_n and its own values — of discrete energy spectrum $\tilde{E}_n$. Treatment of a quantum dot as a deep extended rectangular potential pit V_0 in a perfect crystal structure and Brillouin zones under the conditions when all sizes a of the nanoparticle are smaller than the de Broglie wavelength for electron Λ, makes it possible to use a solution variant for a one dimensional linear case in the form of $\Psi_n \sim 8mV_0(h^2n^2)^{-1}\sin(nx/x_0)$, $\Lambda \sim h[2m(E_g + \tilde{E}_n)]^{-1/2}$, and equation for $\tilde{E}_n$ is in the form of

$$\tilde{E}_n \sim h^2n^2(8mx_0^2)^{-1} \sim 0.35n^2(a^2m/m_0)^{-1}, \qquad (1)$$

where h — Planck constant, a — linear size of quantization area, $n = 1, 2, 3,\ldots$ — quantum numbers; in calculations $\tilde{E}_n$ and E_g are expressed in electron volts, a and Λ — in nanometers.

Stable electron states are selected in a quantum dot that an integer number of half-waves Ψ_n is accommodated in the linear distance of its motion between the QD boundaries. Any influencing energy impact on the electron in QD leads to its transition from one steady state to another. The transition process itself has the nature of charge instability, leading to current instability. The stability of the moving electron state and frequency of its standing wave may mean that its motion between the QD boundaries in this state has a resonant nature. In our case nanocrystals have lattices with parallel planes, and a variant of linear resonant motion of the conduction electron can be considered as a periodically

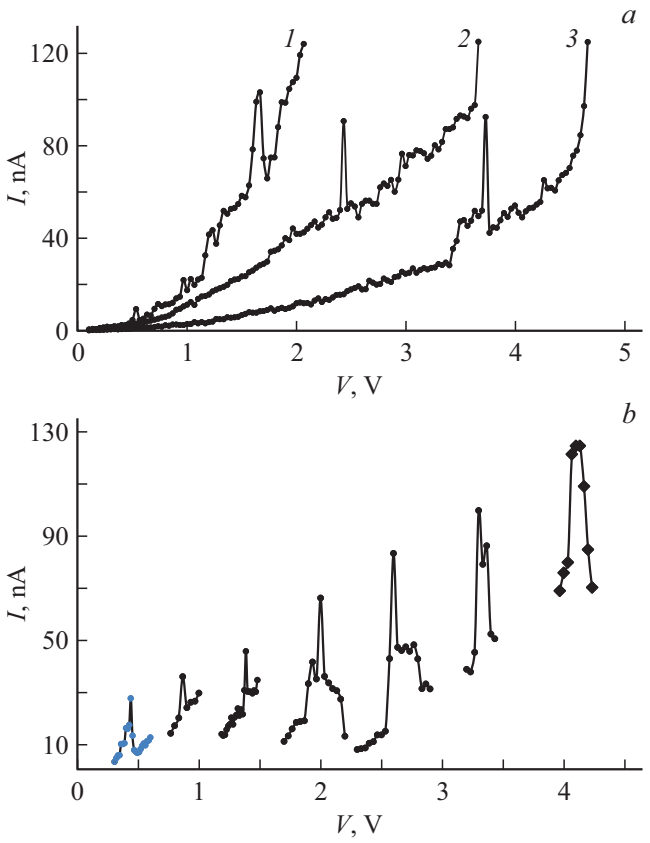

Figure 2. *a* — BAX: *1* — QD-PbS, *2* — QD-HgSe, *3* — QD-InSb; *b* — CVC fragments of QD-InSb.

oscillating process between planes of a parallelepiped with the maximum distance between them equal to one of QD sizes. Thus, one-dimensional nature of electron motion and quantization condition $a \leqslant \Lambda$ result in the fact that in a quantum dot at each moment of time there can be only one electron, and the current process is one-electron (electron-by-electron).

CVC of two types were observed for the investigated samples: with quasi-periodic deviations from monotonicity (fig. 1, *b*) and with surge currents in the form of individual peaks (fig. 2, *a*). Additionally tunnel-current CVC of test samples were measured: ITO layer (curve *5* on fig. 1, *b*) and microparticles InSb (curve *4* on fig. 1, *b*).

We explain first type CVC by the nature of electron motion in QD with dimensions $a \geqslant \Lambda$ within Bloch oscillation model [18]. The main obstacle for their observation is electron scattering on defects of the crystal lattice and phonons. However, in QD with dimensions of $a \sim \Lambda$ the electron moves in a ballistic and, perhaps, quasi-resonant manner, as if it „does not respond“ to the structural interference, and the nature of its motion is determined by quantum selection of pulse in the Brillouin zone. These circumstances may be indicative of a real possibility to observe Bloch oscillations acting in the QD under energy impacts on the electron. The energy step $\Delta V \sim \Delta\tilde{E}$ of such oscillation in CVCs can be calculated by differentiating

Data on electron energy $\tilde{E}_n$ int the stages of current (λ_{vac}) and spectral (λ_{abs}) peaks and values of quantization size a calculated under formula (1)

QD	Parameter	$n=1$			$n=2$			
PbS	$\tilde{E}_n$, eV	0.51	0.87		1.23	1.85	2.6	3.07
	a, nm	3.0	2.4		3.8	3.1	2.6	2.4
	p, %	22	20		32			
	λ_{vac}, nm	1350	969		1377			
	λ_{abs}, nm	1380	1450		1750			
HgSe	$\tilde{E}_n$, eV	0.27	0.65	0.75	1.07	1.43	1.87	2.43
	a, nm	5.4	3.5	3.3	5.4	4.6	4.0	3.6
	p, %	18	17	10	27	17		
	λ_{vac}, nm	3647	1870	1550	1550	1125		
	λ_{abs}, nm	3700	1940	1660	1660			
InSb	$\tilde{E}_n$, eV	0.44	0.87		1.39	2.0	2.6	3.3
	a, nm	7.4	5.6		8.8	7.4	6.4	5.8
	p, %	7	38		24	19		
	λ_{vac}, nm	2030	1192		1185	838		
	λ_{abs}, nm	1960	1250		1660			

equation (1) for the energy of electron as a function of distance: $\Delta\tilde{E} \sim 0.7a^{-3}(m/m_0)^{-1}\Delta a$. If we suggest that Δa is equal to the constant of nanocrystal lattice (QD), we may calculate $\Delta\tilde{E}$ using data produced from curves shown in fig. 1, *b*. For QD-InSb (curve *1* in fig. 1, *b*) $\Delta V \sim \Delta\tilde{E} \sim 0.11$ eV, $a \sim 6.7$ nm; for QD-HgSe (curve *2* in fig. 1, *b*) $\Delta V \sim \Delta\tilde{E} \sim 0.10$ eV, $a \sim 4.5$ nm; for QD-PbS (curve *3* in fig. 1, *b*) $\Delta V \sim \Delta\tilde{E} \sim 0.08$ eV, $a \sim 3.9$ nm.

Current oscillations observed in CVC are the effect of a subtle physical process — charge instability provided for by quantum readjustment under exposure of charge carriers to electric field energy. The general nature of CVC is determined by the motion of an electron inside QD and emission therefrom. As demonstrated in our papers [11,19], such phenomena are due to mechanisms of Coulomb limitation in QD and tunneling through its boundary barriers. Fig. 1, *c* presents CVCs in coordinates that specify current limitation by charge — $I \sim V^{\beta}$. At the same time the found values $\beta \sim (2-2.5)$ comply with the Coulomb current limitation model [11,19].

With applied voltage V from zero and above, the electron injected from the electrode to the QD is transferred to a steady resonant state of $n = 1$. The first current peak V_1 (fig. 2, *a*) manifests itself on CVC. With increase in V the electron is removed from this state by tunneling through the boundary and creating current until the next electron is transferred to the steady resonant state of $n = 2$. At the same time the second current peak V_2 manifests itself on CVC. Appearance of current peaks of the following orders is possible already under the conditions of overbarrier span and potential exceeding work function, and is hardly probable in theory [17].

Fig. 2, *b* presents as an example a sequence of current peaks in the form of CVC fragments for QD-InSb. The table

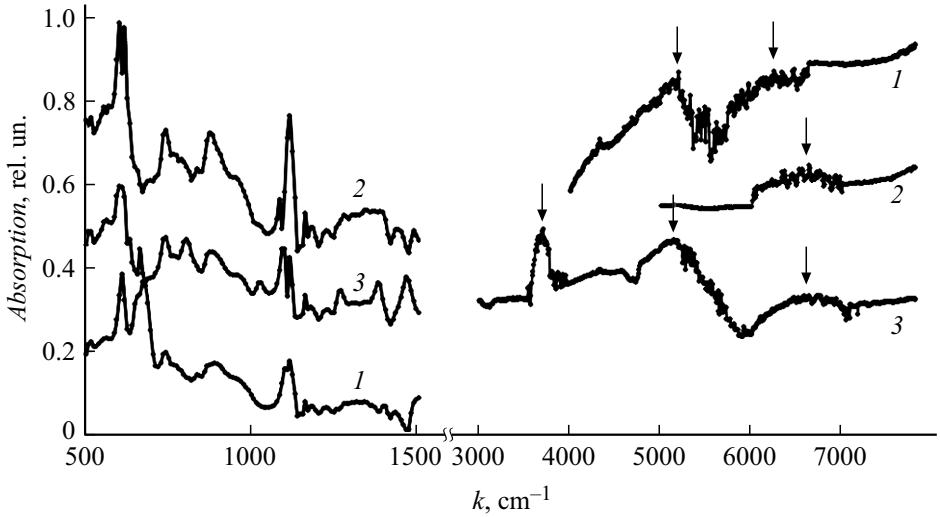

Figure 3. Absorption spectra: *1* — QD-InSb, *2* — QD-PbS, *3* — QD-HgSe.

for all variants presents values of current peak dot voltage V_n and dimensions of quantization distance length a, calculated according to formula (1) in a suggestion that $\tilde{E}_n \sim V_n$. Besides, compliance with ratio $a < \Lambda$ was tested. Besides, percentage p is given for the values of the found parameter a in the total number of CVC samples.

Fig. 3 shows typical absorption spectra of the samples (arrows indicate spectral peaks). Using these results and calculating the electron energy using formula (1) for the quantum dots of each semiconductor enabled us to establish that the spectra were caused by the QD sizes whose distribution has one (distribution *1* in fig. 1, *a*) or two humps (distribution *2* in fig. 1, *a*) [5,20]. In accordance with the dependence of energy on size according to formula (1), the energy (and wavelength) spread should be double of that for a size spread, i. e. in our case $\pm 10\%$, which is estimated and observed for the marked peaks in fig. 3. Therefore, the absorption edge and one or two humps on the curves in fig. 3 are defined as characteristic points for the wavelength values λ. The table presents specific values λ, found from current-voltage (λ_{vac}) and spectral (λ_{abs}) dependences. These values are due to interzone ($n = 1$) and possibly intrazone ($n = 2$) transitions. Besides, variants of high values $\tilde{E}_n$ at $n = 2$ (three right columns of the table) are rare ($p < 10\%$), and corresponding spectral peaks are weakly manifested. Such rare occurrence can be explained by the low probability of stable high-order mode formation, and, in some cases, by small numbers of particles in their dimensional distribution.

In fig. 3, characteristic peaks with intervals of approximately 0.1 eV are observed in the region of extremely long wavelengths. The analysis showed that they can be attributed to intraresonance transitions. In this case, resonance may fail when exposed to quanta with energy less than 0.1 eV, which will lead to zeroing of the corresponding current peaks. All these possible phenomena can be used for photon registration of radiation quanta in the spectral range greater than 10 μm.

Thus, electron passage through a quantum dot as a deep extended potential pit leads to quasi-periodic oscillations and current peaks on CVC with energy (voltage) values correlating with absorption spectra and calculations using the eigenfunction formula of the Schr'dinger equation solution. Such manifestations are defined by the mechanism of size quantization and the state of periodically-oscillating resonance of the electron motion between QD boundaries, while the quasiperiodic modulation can be explained by the model of Bloch oscillations.

Acknowledgments

The authors would like to acknowledge O.Yu. Tsvetkova for sample preparation.

Funding

The research has been conducted with financial support by the Russian Foundation for Basic Research under the scientific project 20-07-00603-A.

Conflict of interest

The authors declare that they have no conflict of interest.

References

[1] D. Porotnikov, M. Zamkov, J. Phys. Chem. C, **124** (40), 21895 (2020). DOI: 10.1021/acs.jpcc.0c06868

[2] M. Alizadeh-Ghodsi, M. Pourhassan-Moghaddam, A. Zavari-Nematabad, B. Walker, N. Annabi, A. Akbarzadeh, Part. Part. Syst. Charact., **36** (2), 1800302 (2019). DOI: 10.1002/ppsc.201800302

[3] S.B. Brichkin, V.F. Razumov, Russ. Chem. Rev., **85** (12), 1297 (2016). DOI: 10.1070/RCR4656.
[4] M.C. Weidman, M.E. Beck, R.S. Hoffman, F. Prins, W.A. Tisdale, ACS Nano, **8** (6), 6363 (2014). DOI: 10.1021/nn5018654
[5] N.D. Zhukov, T.D. Smirnova, A.A. Khazanov, O,Yu. Tsvetkova, S.N. Shtykov, FTP, **55** (12), 1203 (2021) (in Russian). DOI: 10.21883/FTP.2021.12.51706.9704
[6] A.S. Perepelitsa, *Opticheskie svoystva lokalizovannykh sostoyaniy v kolloidnykh kvantovykh tochkakh sulfidov kadmiya i serebra*, kand. dis. (Voronezh. gos. un-t, Voronezh, 2017) (in Russian).
[7] V.P. Dragunov, I.G. Neizvestny, V.A. Gridchin, *Osnovy nanoelektroniki* (Logos, M., 2006) (in Russian).
[8] G. Kirczenow, Phys. Rev. B, **98** (16), 165430 (2018). DOI: 10.1103/PhysRevB.98.165430
[9] A.K. Giri, H.K. Pandey, A.R. Singh, P.R. Singh, Int. J. Eng. Res. Technol., **8** (8), 280 (2019). IJERTV8IS080071
[10] K. Shibata, H. Yuan, Y. Iwasa, K. Hirakawa, Nature Commun., **4**, 2664 (2013). DOI: 10.1038/ncomms3664
[11] N.D. Zhukov, M.V. Gavrikov, V.F. Kabanov, I.T. Yagudin, Semiconductors (2022). DOI: 10.1134/S1063782621040199.
[12] http://xumuk.ru/encyklopedia
[13] D.V. Krylsky, N.D. Zhukov, Tech. Phys. Lett., **46** (9), 901 (2020). DOI: 10.1134/S1063785020090205.
[14] N.D. Zhukov, M.V. Gavrikov, Mezhdunar. nauch.-issled. zhurn., № 8(110), 19 (2021) (in Russian). DOI: 10.23670/IRJ.2021.110.8.004
[15] A.Zh.K. Al-Alvani, A.S. Chumakov, M.V. Gavrikov, D.N. Bratashov, M.V. Pozharov, A.S. Kolesnikova, E.G. Glukhovskoy, Izv. Yugo-Zapad. gos. un-ta. Ser. Tekhnika i tekhnologii, **9** (1), 56 (2019) (in Russian).
[16] F.A. Serrano, S.-H. Dong, J. Quantum Chem., **113** (20), 2282 (2013). DOI: 10.1002/qua.24449
[17] V.N. Davydov, O.F. Zadorozhny, O.A. Karankevich, Russ. Phys. J., **62** (3), 499 (2019). DOI: 10.1007/s11182-019-01737-5.
[18] R.A. Suris, I.A. Dmitriev, Phys. Usp., **46** (7), 745 (2003). DOI: 10.1070/PU2003v046n07ABEH001608.
[19] N.D. Zhukov, M.V. Gavrikov, D.V. Kryl'skii, Tech. Phys. Lett., **46** (9), 881 (2020). DOI: 10.1134/S106378502009014X.
[20] N.D. Zhukov, S.A. Sergeev, A.A. Khazanov, I.T. Yagudin, Pisma v ZhTF, **47** (22), 37 (2021). DOI: 10.21883/PJTF.2021.22.51725.18927